Macromolecules
ARTICLE

Macromolecules **2010**, *43*, 10545–10553 **10545**
DOI: 10.1021/ma102036h

Nonisothermal Crystallization Behaviors of Nanocomposites Prepared by *In Situ* Polymerization of High-Density Polyethylene on Multiwalled Carbon Nanotubes

Jihun Kim,[†] Soonjong Kwak,[‡] Soon Man Hong,[‡] Jae Rock Lee,[§] Atsushi Takahara,[⊥] and Yongsok Seo*[,†]

[†]*Intellectual Textile Research Center (ITRC) & School of Materials Science and Engineering, College of Engineering, Seoul National University, Shillimdong 56-1, Kwanakgu, Seoul, Korea 151-744,* [‡]*Polymer Hybrid Research Center, Korea Institute of Science and Technology, P.O. BOX 131, Cheongryang, Seoul, Korea 136-791,* [§]*Energy Materials Research Center, Korea Research Institute of Chemical Technology, P.O. BOX 107, Yousungku, Taejon, Korea 305-600, and* [⊥]*Institute for Materials Chemistry & Engineering, Kyushu University, 744 Motooka, Nishiku, Fukuoka 819-0395, Japan*

Received September 1, 2010; Revised Manuscript Received November 3, 2010

ABSTRACT: Thermal properties and nonisothermal crystallization kinetics of polyolefin nanocomposites (high-density polyethylene/multiwalled carbon nanotubes) were characterized by differential scanning calorimetry and thermogravimetric analysis. *In situ* metallocence polymerization was used to prepare nanocomposites of multiwalled carbon nanotubes (MWCNTs) and high-density polyethylene (HDPE). This polymerization method consists of attaching a metallocene catalyst complex onto the surface of the MWCNTs followed by surface-initiated polymerization to generate polymer brushes on the surface. A kinetic equation for the nonisothermal crystallization was employed to analyze the crystallization characteristics of the nanocomposites. The Avramic exponent, *n*, can be reasonably well determined from the nonisothermal crystallization exotherm. The polarized optical microscopy showed that neat polyethylene possessed a well-developed spherulite morphology, whereas the nanocomposites displayed elongated entities that subsequently developed as bundlelike entities. Nonisothermal analysis implicitly provides clues about the morphological development history and HDPE molecular ordering around the carbon nanotubes.

Introduction

Carbon nanotubes (CNTs) have attracted a great deal of interests during the past two decades as a promising filler in polymer-based nanocomposites because of their special properties such as low mass density, huge surface to volume ratio, large aspect ratio, extremely high tensile modulus and tensile strength, high thermal conductivity, and high electrical properties.[1−5] Owing to the exceptional intrinsic properties of the filler particles, novel materials have been envisaged, which could exhibit unprecedented property enhancements, in particular, at filler loadings much lower than in conventional composite technology.[6,7] In the field of thermoplastic nanocomposites, the reported property enhancements include improved mechanical performance, high thermal and electrical conductivity, increased crystallization rate, and altered rheological behavior.[8−13] Previous studies have indicated that nanocomposite performance depends on both intrinsic properties of carbon nanotubes such as the purity of the carbon nanotube, diameter, length, aspect ratio, and the type of carbon nanotube as well as composite characteristics, including nanotube dispersion and alignment in the polymer matrix and polymer structure.[14−19] Therefore, the successful development of promising MWCNTs/polymer nanocomposites to a large extent depends on the ability to disperse the MWCNTs homogeneously in the polymer matrices and to ensure strong MWCNT−polymer interfacial adhesion for good stress transfer.[20−24]

The homogeneous dispersion of carbon nanotubes is not easy to achieve, especially in nonpolar polymer matrices such as polyolefin because carbon nanotubes tend to form aggregates that are thermodynamically stabilized by van der Waals forces and numerous $\pi-\pi$ interactions between the tubes. Various methods have been used to disperse these aggregates such as ultrasonification, use of surfactant, chemical functionalization of the nanotube surface, and *in situ* polymerization.[25] *In situ* polymerization is a promising approach for the preparation of polyolefin nanocomposites without deteriorating the intrinsic properties of MWCNTs. Recently, *in situ* polymerization has been performed by many researchers for the fabrication of polyolefin nanocomposites containing carbon nanotubes using not only a supported Ziegler−Natta catalyst but also a supported metallocene catalyst.[8−13,26,27] Because the catalyst was physicochemically grafted to the carbon nanotube surface, individual carbon nanotubes were homogeneously coated by polymer chains that grow on the surfaces, preventing carbon nanotubes from aggregating. The product can be used directly or as a master batch for future nanocomposites.[13,16]

Polyethylenes are the most widely used polyolefin-based thermoplastics. In light of the large spectrum of their applications, improvements and technical breakthroughs in these materials can yield significant economic impact.[27] In our previous study, we reported the preparation of nanocomposites of multiwalled carbon nanotubes (MWCNT) and high-density polyethylene (HDPE) by *in situ* metallocence polymerization and their electrical conductivity and rheological response.[28] Electrical conductivity and rheological properties showed the property transition (sudden drastic increase) at the critical concentration of carbon nanotubes (percolation threshold). Differences in the percolation behaviors between the MWCNT-mixed nanocomposites and the

*To whom all correspondence should be addressed. E-mail: ysseo@snu.ac.kr.

Published on Web 11/23/2010

PE-coated MWCNT nanocomposites were ascribed to the difference in the dispersion and the tube−tube distance between MWCNTs. As a part of our continuous efforts to investigate the physical properties of the nanocomposites, the present work provides a direct comparison between the achieved performance levels after incorporation of nanotubes on additional fronts, i.e., thermal behavior and crystalline morphology. Because the addition of fillers significantly affects the crystallization behavior and resulting crystalline morphology of the matrix, this highly oriented columnar morphology of the composites, extending over the entire fiber−matrix interface, is expected to be considerably different from the spherulitic crystal growth commonly encountered in HDPE.[25]

For the crystallization kinetics, isothermal crystallization is normally analyzed using Avrami's equation. In an isothermal crystallization experiment, however, it is difficult to maintain the melted sample in an amorphous state while cooling it to the crystallization temperature. Moreover the crystallization processes encountered in nature tend to be nonisothermal. Nonisothermal crystallization kinetics has been theoretically explored by Ozawa,[29] who extended the mathematical derivation proposed first by Evans.[30,31] However, Ozawa's theory has some limits.[32,33] Because this approach compares the degrees of conversion at a fixed temperature for various cooling rates, it can lead to deviations from the predicted linear behavior. We recently devised an analysis scheme to avoid the problem of the Ozawa analysis.[34,35] The nonisothermal crystallization kinetics can provide supplementary information about the crystal structure when analyzing crystallization. It may give additional insight into the crystallite structures produced during nanocomposite formation. Hence, the objective of the present study is to apply our previously proposed nonisothermal analysis method[35] to the crystallization behavior of a pristine polyethylene and *in situ*-formed nanocomposites, focusing on the morphological changes that occurred due to the existence of MWCNTs, and to investigate the thermal properties of *in situ* polymerized HDPE/MWCNT nanocomposites.

Experimental Section

Materials. Multiwalled carbon nanotubes (MWCNT) were supplied by Iljin Nanotech Co. (Korea). MWCNTs prepared by a thermal chemical deposition method were used without pretreatment. MWCNT rather than single-walled carbon nanotubes (SWCNT) were used due to the formation of less dense bundles of entangled nanotubes, allowing more catalyst (methylaluminoxane) to reach the inside of the bundles in the solvent than SWNTs.[18,19] The tube diameter is in the range 10−15 nm, and length is in the range 10−20 μm. The MWCNTs were dried in a vacuum oven for more than 24 h at 60 °C before use.

Because the preparation of HDPE/MWCNT nanocomposites by the *in situ* polymerization of polyethylene on MWCNTs whose surfaces were impregnated by the metallocence catalyst was fully reported elsewhere,[28] we will only reiterate the procedure. Ethylene (Dong-A Co., 99.9%) was used as a polymerization monomer, and dichloro[*rac*-ethylenebis(indenyl)]zirconium(IV) (*rac*-Et(Ind)$_2$ZrCl$_2$) was used as a catalyst. Methylaluminoxane (MAO, 10 wt % solution in toluene), a commonly used cocatalyst in metallocene-based olefin polymerization, was also used. All manipulations of the compounds were carried out using a vacuum line, standard Schlenk or cannula techniques under dry argon, and a glovebox. After we determined the saturated concentration of MAO supported on the surface of the MWCNTs, we fixed the catalyst on the surface of the MWCNTs. The polymerization reactions were performed in a 5 L high-pressure reactor equipped with a magnetic stirrer. Dried MWCNTs were charged first into the reactor and added to purified toluene. The MWCNT dispersion was done by a sonic treatment for 90 min at room temperature. After the sonic treatment, a triisobutylaluminum (TIBA) solution was added to the reactor as a scavenger, and then MAO was injected into the slurry. The catalyst fixation was done for 1 h at 40 °C. Then, *rac*-Et(Ind)$_2$ZrCl$_2$ was introduced into the reactor. The activation reaction of the MWCNTs was performed for 1 h at 50 °C. Injecting ethylene started the polymerization. The polymerization reaction was carried out under a constant pressure of 4 bar of ethylene at 50 °C. After a predetermined reaction time, the polymerization was quenched with a diluted HCl solution in methanol. The polymer was precipitated in methanol, filtered, and dried in a vacuum oven.

Characterization. Thermal properties of the nanocomposite samples were analyzed using differential scanning calorimetry (DSC), performed on a Mettler DSC 30. Prior to analysis, the samples were dried at 80 °C in a vacuum oven for 24 h. Approximately 45 mg of the dried composites was used in each run. To examine nonisothermal crystallization, the samples were heated from 25 to 200 °C at a heating rate of 10 °C/min and then cooled at different cooling rates. Thermogravimetric analysis (TGA) was performed on a TA Instruments (TA Q50) under a nitrogen atmosphere with a heating rate of 20 °C/min in a temperature range of 50−650 °C.

A polarized optical microscope (POM) (Olympic BH-2) equipped with a Mettler FP82 HT hot stage and a CCD camera was used to measure the growth rate of the crystallites. The morphological observations were performed by scanning electron microscopy (SEM). SEM observations were performed on a Hitachi S-4700 microscope, and the samples were coated with platinum in a C-1045 ion sputter coater.

Description of the Theoretical Model

Here, we briefly present the basic equations from our earlier report.[34,35] In the Ozawa equation, the Avrami equation is expressed using a cooling rate, as expressed in the following equation:

$$\ln[-\ln(1-x_v(T)_U)] = \ln K(T) - n \ln U \quad (1)$$

where $x_v(T)$ is the volume fraction of the polymer transformed at a temperature T and the cooling rate U, and $K(T)$ is the so-called cooling function, which only varies as a function of the temperature. Because the Ozawa equation is based on the volume fraction of the crystallites, conversion of the weight fraction of the polymer, $x_w(T)$, to the volume fraction of the polymer, $x_v(T)$, is needed. This can be easily done by using the density of the amorphous phase and the density of the crystallized phase.[34,35] As suggested by the theory, a linear dependence between ln $K(T)$ and the temperature T is assumed, such that $\ln K(T) = aT + b$. When the temperature reaches the peak of the exothermal curve, T_{max}, for a given cooling rate, the first and the second derivatives of the curve with respect to the temperature should be zero. Using eq 1 with this condition, a linear relation between T_{max} and ln(U) can be obtained, i.e., $n \ln (U) = aT_{max} + b - \ln[-\ln(1 - x_v(T_{max})_U)]$. Therefore, eq 1 can be rewritten as the following:

$$\ln[-\ln(1-x_v(T)_U)] = a(T - T_{max}) + \ln[-\ln(1-x_v(T_{max})_U)] \quad (2)$$

Hence, the value of the parameter a can be estimated from the slope of a plot of $\ln[-\ln(1 - x_v(T)_U)]$ against $T - T_{max}$. In addition, plotting T_{max} versus ln(U) gives a straight line whose slope is n/a and intercept is $(\ln[-\ln(1 - x_v(T_{max})_U)] - b)/a$; thus, all of the parameters can be determined without resorting to any numerical process.[34,35]

Results and Discussion

Thermal Properties and Nonisothermal Crystallization Kinetics. We successfully prepared polyethylene (PE)/multiwalled carbon

Table 1. Experimental Conditions for the PE/MWCNT Nanocomposites Using *in Situ* Polymerization of Ethylene and Corresponding Polymerization Results

	MWCNT (g)	Al/Zr	MAO (mmol)	polymerization time (min)	filler content (wt %)	M_w	PDI
homo PE		500	20	150	0	108 647	6.23
PE/MWCNT(1.5)	0.6	500	4.2	150	1.5	225 968	4.35
PE/MWCNT(2.4)	1	500	7	150	2.4	198 507	2.84
PE/MWCNT(3.5)	3	500	21	150	3.5	130 426	4.25
PE/MWCNT(7.3)	5	500	30	150	7.3	93 350	5.95
PE/MWCNT(8.8)	7	500	30	150	8.8	93 305	4.10
PE/MWCNT(10.9)	9	500	30	150	10.9	129 151	4.90
PE/MWCNT(12.4)	15	500	30	150	12.4	128 195	5.38

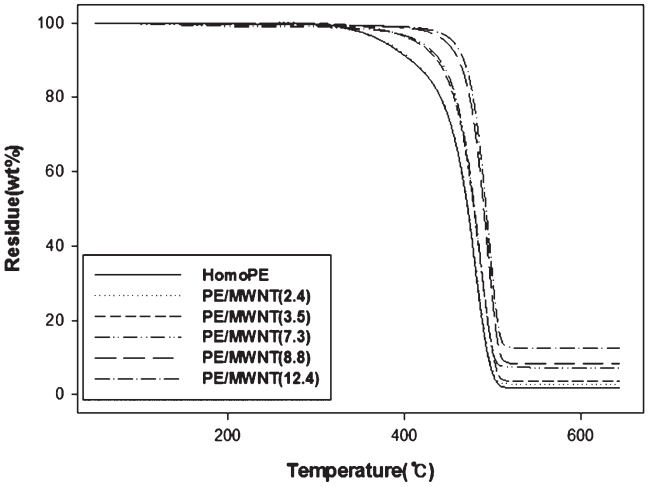

Figure 1. TGA graphs for homo PE, PE/MWCNT(2.4 wt %), PE/MWCNT(3.5 wt %), PE/MWCNT(7.3 wt %), PE/MWCNT(8.8 wt %), and PE/MWCNT(12.4 wt %).

nanotube (MWCNT) nanocomposites with various weight fractions using *in situ* metallocene polymerization.[28] Table 1 summarizes the experimental conditions for the catalyst preparation and polymerization results. Although nanocomposites with a variety of MWCNT concentrations were synthesized, two samples containing 1.5 wt % MWCNT and 2.4 wt % MWCNT were mainly used in this study to see the effect of MWCNT addition on the thermal properties.

Thermal degradation characteristics of HDPE/MWCNT nanocomposites by TGA are shown in Figure 1. It is known that the thermal degradation of polyethylene occurs by chain scission.[37] At temperatures in excess of ~400 °C, the C−C bonds of the polyethylene backbone spontaneously break to yield two shorter chains, each of which is furnished with a terminal radical. Once the terminal radicals have been produced, they may undergo "backbiting" reactions. Backbiting results in the emission of low molecular weight alkanes and alkenes.[37] Carbon nanotubes have high electron affinities due to many π electrons similar to C_{60}; whereby, it has been proposed to act as a scavenger of free radicals.[38] Thermal stabilities (onset temperature, degradation temperature) were dramatically enhanced with the MWCNT addition. An increase in the degradation temperature as high as 50 °C was achieved for PE/MWCNT (12.4) in a N_2 atmosphere. A similar result regarding the stabilities of PE/CNT nanocomposites was reported by Li et al.:[25] however, this was much higher than the result by Watt et al., who achieved approximately an 18 °C increase in the degradation temperature of PE in N_2 with ~14 wt % MWCNTs.[38] The difference is attributable to the different mixing procedure. Watt et al. used a melt blending method while Li et al. used a solution blending method. We used the *in situ* polymerization method. This result implies that good dispersion and enhanced interfacial adhesion between MWCNT could hinder the flux of degradation products and, finally, delay the onset of degradation. The degradation temperature of MWCNTs is known to be approximately 600−700 °C in the air, and the thermal conductivity of the MWCNT is known to be above 1500 W m^{-1} K^{-1}.[28] MWCNTs act like inorganic fillers, but due to the strong adhesion between PE molecules and the nanotube walls, thermal energies were well transferred to the carbon nanotubes to delay the onset of the composite degradation.

DSC scans can be seen in Figure 2. All of the samples were cooled from the melt temperature (200 °C) with various cooling rates. All of the samples exhibit a single crystallization exotherm. The main changes are in the characteristic onset and peak crystallization temperatures, i.e., in the values of the associated enthalpies and the peak broadening effects in the nanocomposites compared to neat HDPE. We can see that the onset temperatures of the nanocomposites are higher than those of neat HDPE, which implies that for all *in situ* polymerized nanocomposite samples the supercooling necessary for the crystallization was much lower. This result is a direct consequence of the remarkable nucleation effect caused by the MWCNTs. Therefore, the crystallization temperature increases with MWCNT content as a result of the nucleating action of MWCNT.[13,25,37] T_{max} of the nanocomposites is higher than that of the homo HDPE at all cooling rates, implying that MWCNT act as nuclei to induce heterogeneous nucleation. The fact that HDPE/MWCNT (2.4 wt %) composites exhibit nearly the same crystallization temperature indicates that 1.5 wt % MWCNT provides sufficient (or more than sufficient) nucleation sites, eliminating nucleation as a rate-limiting step.[38]

As we pointed out earlier, Ozawa's approach compared the rates of conversions at various temperatures, which could lead to substantial curvature in the Ozawa plot because the crystallization processes at different cooling rates can be at different stages.[34] On the other hand, the current approach can select the relative crystallinity at the same cooling rate and does not include values from other rates, thus safely excluding the possibility of comparison at different stages.[38] The validity of our approach has been exemplified in our previous reports.[34,35] Figure 3 displays a linear variation of the maximum temperature of the crystallization isotherm, T_{max}, of HDPE and the nanocomposites with the logarithm of the cooling rates (ln(U)). The predicted behavior is observed in all cases provided the cooling rate is low (< 7 °C/min). Because less time is available for crystallization at higher cooling rates, T_{max} decreases as the cooling rate increases. T_{max} of the nanocomposites was higher than that of the neat PE at the same cooling rate, indicating a faster crystallization.

The changes in the HDPE crystallinity were obtained after the normalization by dividing the heat flow axis by the weight of the HDPE content in the sample. The relative crystallinity development of neat PE and nanocomposites of 1.5 wt % MWCNT and 2.4 wt % MWCNT is shown in Figure 4. As the cooling rate increases, a large fraction of the

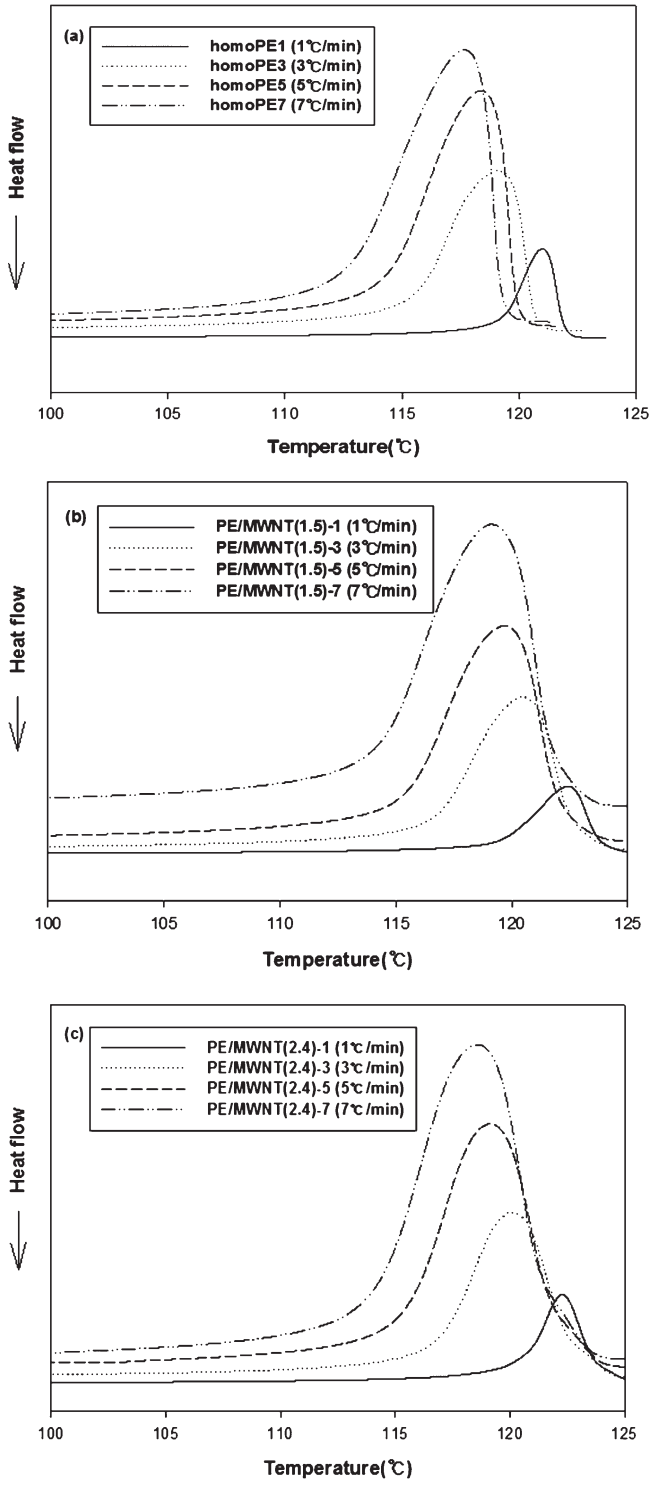

Figure 2. DSC curves of nonisothermal crystallization at different cooling rates: (a) homo HDPE, (b)HDPE/MWCNT(1.5 wt %) nanocomposite, and (c) HDPE/MWCNT(2.4 wt %) nanocomposite.

relative crystallinity occurs after the most rapidly increasing point in the heat flow curve during which the kinetics change to a slower process. Inclusion of more MWCNTs resulted in an increase in the degree of crystallinity (Table 2). Considering the large aspect ratio and surface-to-volume ratio of MWCNTs and that most PE molecules are grown vertically from the surface, the crystallinity of the composites would increase with the concentration of the MWCNT. However, excessive addition of MWCNTs creates a large interface

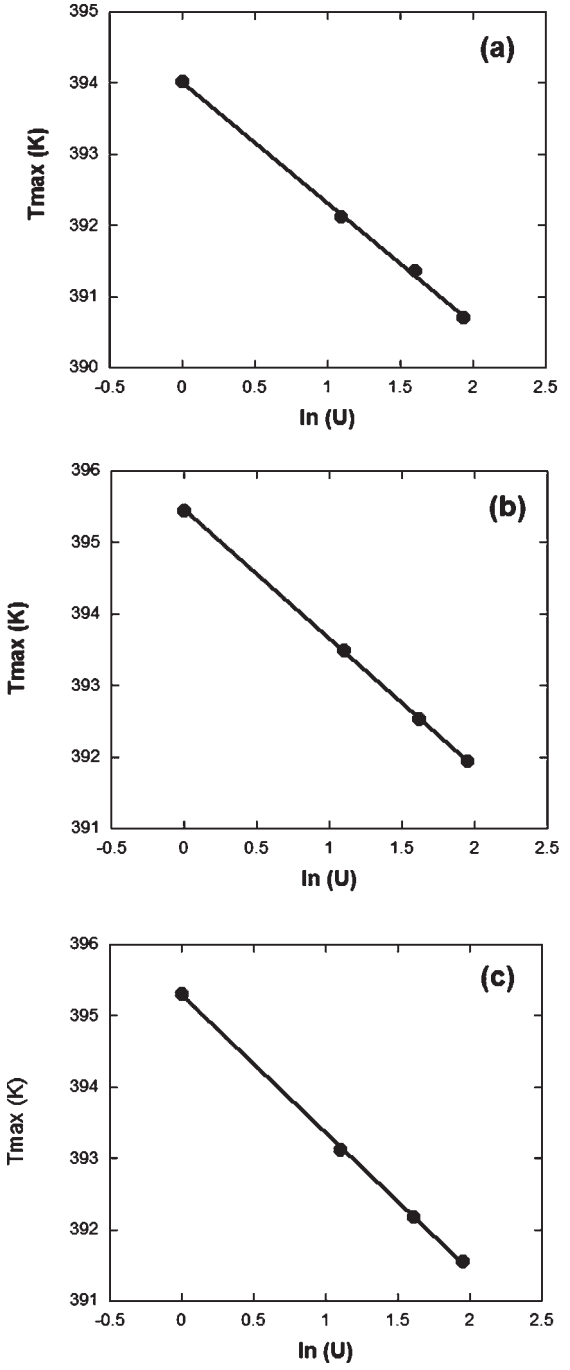

Figure 3. Evolution of T_{max} as a function of ln(U): (a) homo PE, (b) 1.5 wt % PE/MWCNT nanocomposite, and (c) 2.4 wt % PE/MWCNT nanocomposite.

between the PE molecules that surround the MWCNTs and those that are grown vertically from the surface of MWCNTs. The interface region forms an amorphous phase and interferes with crystal growth. Thus, the total crystallinity of the composites decreased when the MWCNT concentration was 12.4 wt % (Table 2). The presence of MWCNTs markedly influences the crystallization behavior of HDPE because MWCNTs produced a higher number of stable crystals while PE chains were grown on the surface of the MWCNTs. In Table 2, the melting temperatures of the composites are presented after the second heating. In spite of the increase in the content of MWCNTs, T_m does not show any noticeable changes. This indicates that the presence of MWCNT has no influence on the lamella thickness of the PE chains.[25]

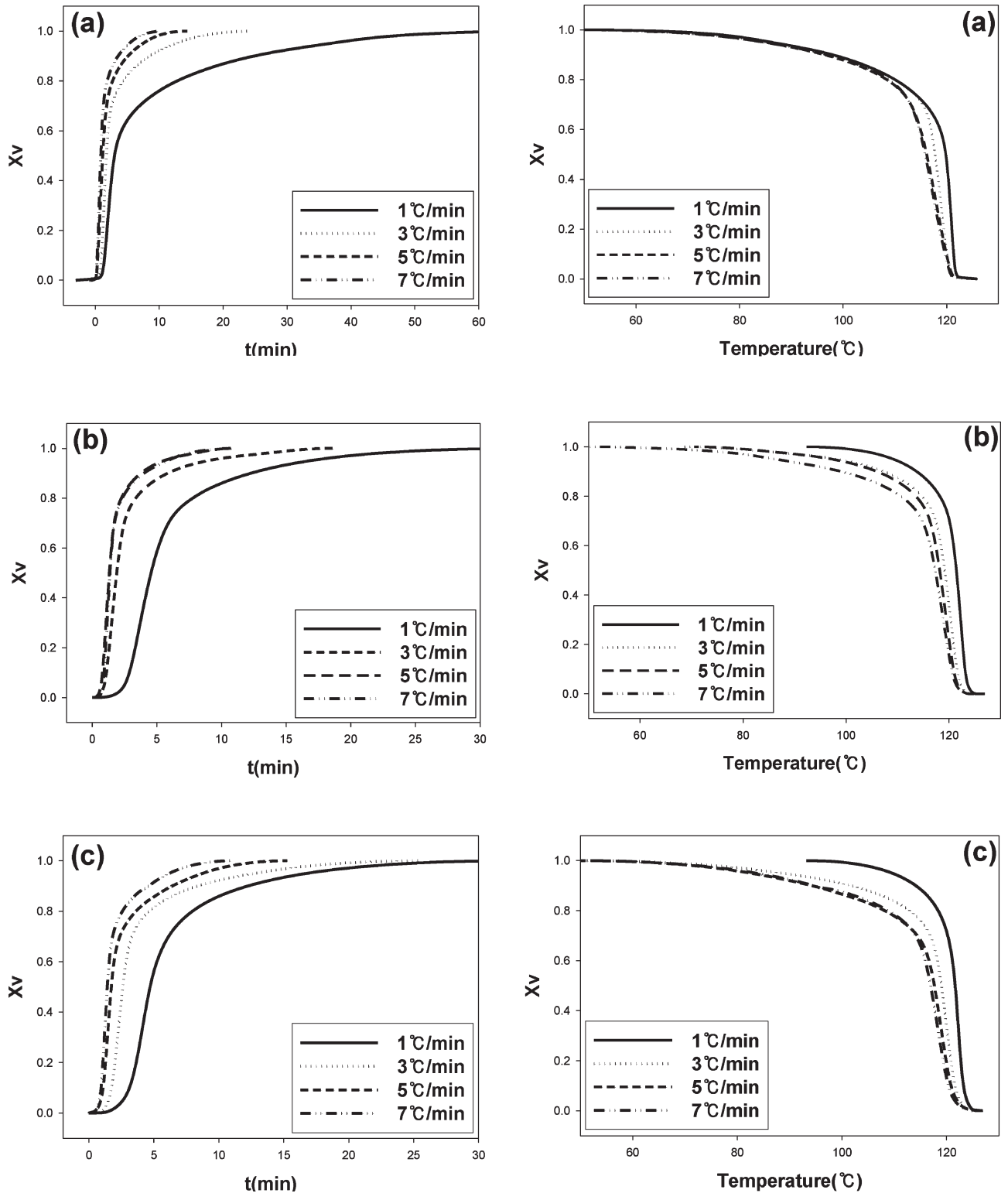

Figure 4. Development of relative crystallinity, X_v, as a function of time (left column) and temperature (right column) at different cooling rates: (a) homo PE, (b) 1.5 wt % PE/MWCNT nanocomposite, and (c) 2.4 wt % PE/MWCNT nanocomposite.

Independent of the crystallization process, the melting temperatures are constant, and the overall crystallinity increases with MWCNT content. However, excessive MWCNT content provides more area for an amorphous interface between HDPE molecules surrounding different MWCNTs that results in the reduction in the crystallinity. The plot of $\ln[-\ln(1 - x_v(T)_U)]$ versus $(T - T_{max})$, shown in Figure 5, gives a straight line with a slope of n/a. The calculated values of the Avrami exponent, n, for neat PE are between 2.6 and 2.9, with an average value of 2.8 (Table 3). This value is close to the characteristic value for spherulitic development arising from athermal instantaneous nucleation.[39] These findings suggest that spherulites are developed during nonisothermal crystallization of the HDPE homopolymer, which, as will be shown later, is consistent with the morphological data. The variation of T_{max} as a function of $\ln(U)$ for the nanocomposites also shows an excellent linear

Table 2. DSC Data for Homo PE, PE/MWCNT(2.4 wt %), PE/MWCNT(3.5 wt %), PE/MWCNT(7.3 wt %), PE/MWCNT(8.8 wt %), and PE/MWCNT(12.4 wt %)

sample	filler content (wt %)	T_m (°C)	crystallinity (%)
homo PE		136.15	64.78
PE/MWCNT(1.5)	1.5	136.07	65.29
PE/MWCNT(2.4)	2.4	136.00	66.2
PE/MWCNT(3.5)	3.5	136.60	68.67
PE/MWCNT(7.3)	7.3	137.22	69.16
PE/MWCNT(8.8)	8.8	136.68	74.12
PE/MWCNT(12.4)	12.4	136.10	71.29

relationship between T_{max} and ln(U) at low cooling rates. Consistent with the behavior of T_{max}, the relative crystallinity data again indicates that the nanocomposites crystallize faster than the neat PE, especially at higher cooling rates. The calculated average value of the Avrami exponent, n, from Figure 4 is ~2.56 for HDPE/MWCNT (1.5 wt %) nanocomposite, 1.99 for HDPE/MWCNT (2.4 wt %) nancomposite, and 1.78 for HDPE/MWCNT (7.3 wt % close to that of the percolation threshold[28]) nancomposite (Table 3). The n values approaching 2 indicate that the encapsulation of MWCNTs by *in situ* polymerization obviously causes heterogeneous nucleation and creates the growth mechanism of the 2-dimensional rod shape.[40]

Morphology of the Nanocomposites. The presence of MWCNT dramatically increases the number of nucleation sites and thereby decreases the average size of crystallites as detected by polarized optical microscopy (Figures 6 and 7). In the absence of MWCNT, HDPE forms large spherulites (20−50 μm) with slightly twisted lamellae. In contrast, the crystal structure in HDPE/MWCNT (1.5 wt %) composites consists of much smaller crystallites (1−5 μm). Because of the excessive nucleation sites in HDPE/MWCNT composites, the crystallites did not grow as large compared to those in neat HDPE molecules. This result is consistent with Winey et al.; however, the preparation methods are different.[6] The half-crystallization time ($t_{1/2}$), which is the time required to accomplish 50% of the crystallization under crystallization conditions, can be obtained from Figure 4. The $t_{1/2}$ values at various cooling rates are also listed in Table 3. The $t_{1/2}$ values decrease with an increasing cooling rate due to faster crystallization. On the other hand, when compared with homo PE, the $t_{1/2}$ values of the nanocomposites increase uncharacteristically with increasing contents of MWCNTs. For solution crystallized composites, the half-time of crystallization is reduced with the inclusion of MWCNTs. Grady et al.[14] also observed in nanocomposites of polypropylene and SWCNT functionalized with octadecylamine that the half-time of crystallization of polypropylene was reduced by a factor of ~2 at both 0.6 and 1.8 wt % SWCNT loading. However, those values are for free polymer molecules crystallized in solution. The HDPE molecules in this study are rooted on the MWCNTs surface, such that they cannot move freely to accommodate the low-energy conformation in the crystalline state. Rather, the HDPE molecules should overcome the entropic penalty of rooting on the MWCNT surface, which would hinder the free-chain conformation. This concept is explained in Scheme 1. At the beginning of the process, faster crystallization proceeds due to the nucleating action of the MWCNT surface. However, after the T_{max}, the PE molecules constrained by rooting on the MWCNT surface for further growth. Thermograms in Figure 2 show that the thermal curves are asymmetric, which means more crystallization occurs after T_{max}. Lower temperature portions than T_{max} are larger than higher temperature portions. The fwhm (full width at half-maximum) increases for the nanocomposites. The interface between each HDPE molecules rooted to different MWCNTs forms amorphous part. Thus, the half-crystallization time increased with MWCNT inclusion. Because of the restriction of space and less freedom in the conformation, it takes more time for the HDPE molecules to become ordered. Rooting on the surface at a later stage restricts the movement of the molecules and decelerates the crystallization kinetics of HDPE.

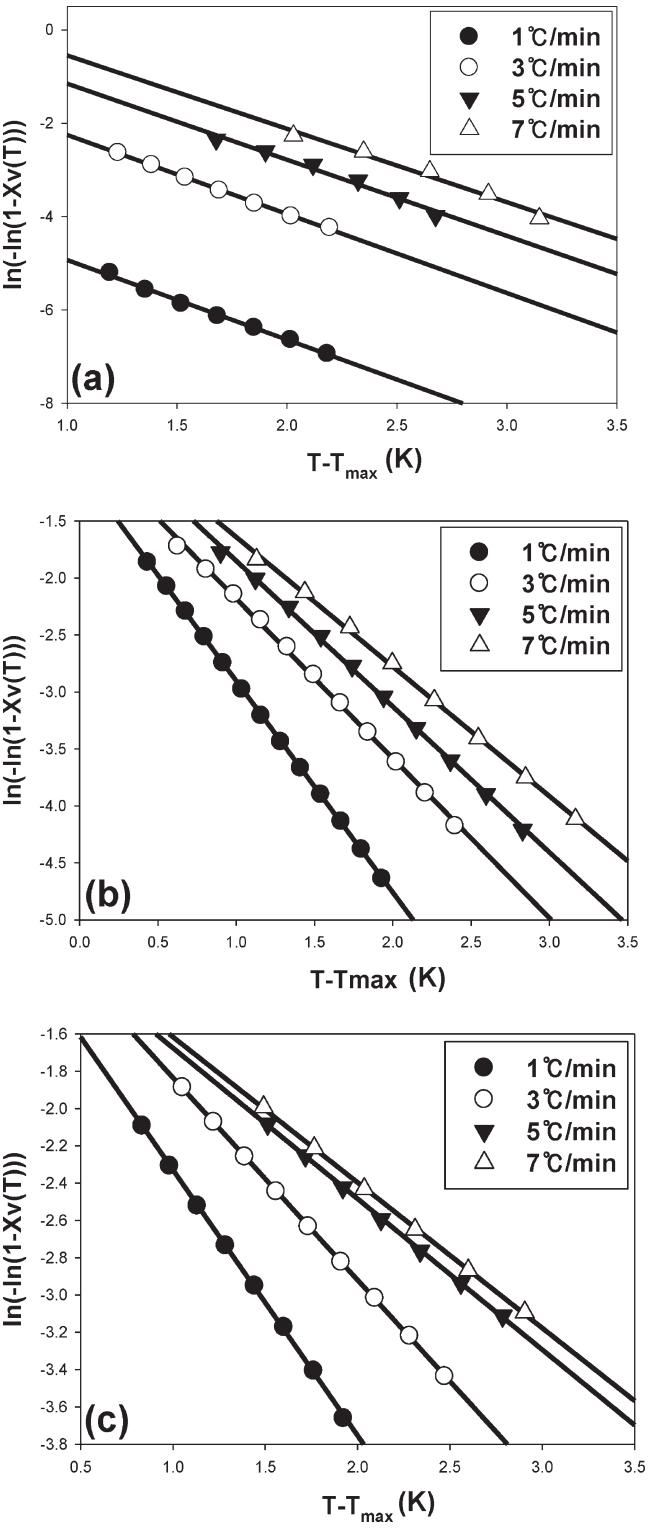

Figure 5. Plot of ln[−ln(1 − $X_v(T)$)] versus $T - T_{max}$ at different cooling rates: (a) homo PE, (b) 1.5 wt % PE/MWCNT nanocomposite, and (c) 2.4 wt % PE/MWCNT nanocomposite.

Table 3. Half-Crystallization Time $t_{1/2}$ and Parameter Values of n

	homo PE		PE/MWCNT(1.5)		PE/MNT(2.4)		PE/MWCNT(7.3)	
cooling rate (°C/min)	$t_{1/2}$	n	$t_{1/2}$	n	$t_{1/2}$	n	$t_{1/2}$	n
1	3.87	2.89	4.55	3.35	4.71	2.76	9.47	2.21
3	1.76	2.87	1.9	2.53	1.94	2.11	3.86	1.83
5	1.18	2.76	1.32	2.31	1.73	1.57	2.27	1.71
7	0.87	2.66	1.05	2.05	1.42	1.51	1.83	1.38
avg		2.80		2.56		1.99		1.78

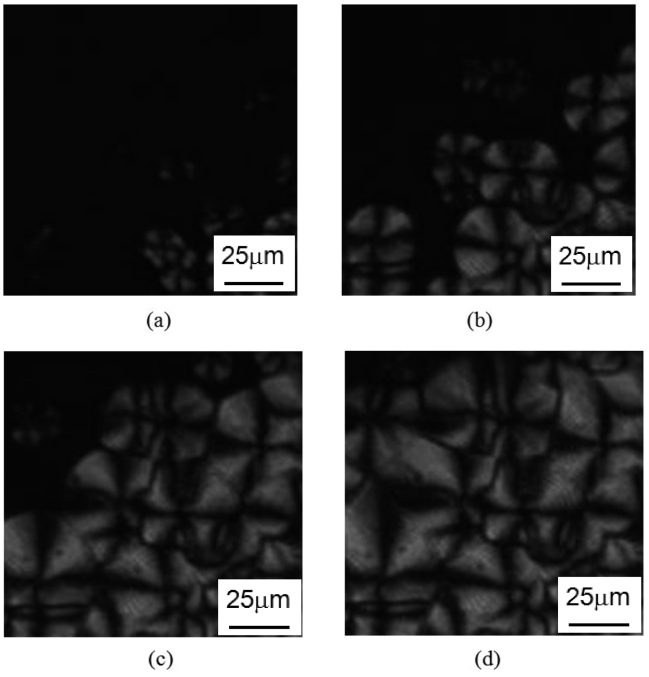

Figure 6. POM images of homo PE at cooling rate, 3 °C/min: (a) 118, (b) 117, (c) 116, and (d) 115 °C (magnification ×400).

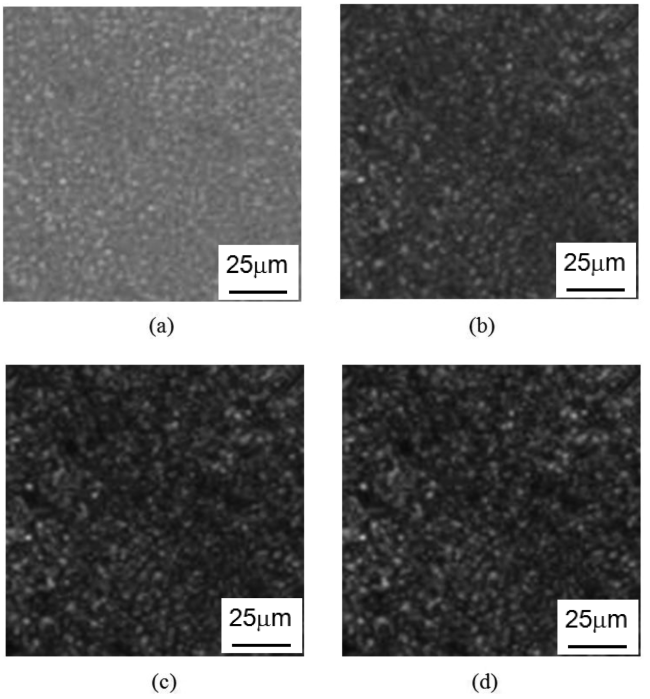

Figure 7. POM images of PE/MWCNT(1.5 wt %) at a cooling rate of 3 °C/min: (a) 118, (b) 117, (c) 116, and (d) 115 °C (magnification ×400).

For the nonisothermal crystallization process, the activation energy of crystallization was derived from the Kissinger equation in the following form:[41,42]

$$\frac{\mathrm{d}[\ln(U/T_{\max}{}^2)]}{\mathrm{d}(1/T_{\max})} = -\frac{E_a}{R} \tag{3}$$

where R is the ideal gas constant and E_a is the activation energy (enthalpy change for the crystallization). Figure 8 shows the correlation between those two. The activation energy derived from the slope of the line is 763 ± 10 kJ/mol for homo PE, 733 ± 13 kJ/mol for PE/MWCNT(1.5 wt %), and 677 ± 6 kJ/mol for PE/MWCNT(2.4 wt %). These results suggest that the introduction of MWCNTs into PE lowers the activation energy and enables the HDPE molecules to be more easily crystallized by heterogeneous crystallization. The presence of MWCNTs dramatically increases the number of nucleation sites and, thereby, decreases the average crystallite sizes as detected by polarized optical microscopy (Figures 6 and 7). Because of the excessive nucleation sites in HDPE/MWCNT composites, the crystallites did not grow as large as the neat HDPE molecules. Agarwal et al.[43] found that MWCNTs can nucleate the crystallization of poly(ethylene terephthalate) at concentrations as low as 0.03 wt %. Recent experiments have shown that, in addition to the nucleating effect, MWCNTs are very efficient in templating polymer lamellae to grow perpendicular to the MWCNT surface in a shish-kebab fashion even under quiescent conditions.[25,27,44] According to the reported results, shear has a minor effect on the crystallization kinetics because of the power of MWCNTs as nucleating agents.[44] Interestingly, Li et al. have patterned polymeric materials periodically on individual carbon nanotubes, resulting in nanohybrid shish-kebab (NHSK) structures, in which a single MWCNT is regarded as the shish.[25,45] These reports imply that MWCNTs alone can induce the orientation of polymer chains without the imposition of flow (shear, elongational, or mixed flow) which is generally applied to incur formation of oriented crystals.[25,45] Winey et al.[6] also found the formation of fiberlike nucleation precursors (or mesophase) at an early stage of crystallization which is the indication of oriented lamellar structures. These precursors were oriented in chain clusters or bundles above a critical size. Polymer preordering comprises intermolecular positional, orientational, and intramolecular conformational order. Therefore, the process of the nanocomposite crystallization consists of polymer chains that go through a conformational adjustment and an orientational transformation, which favors the formation of crystallites. The process also involves the induction time, defined as the time required to detect a significant increase in conversion relative to the initial stage, which decreases with the MWCNT concentration (Scheme 1).[12,25,44]

Very recently, Li et al.[45] reported the surface-induced conformational order of poly(L-lactide) (PLLA) on carbon nanotubes. Using FTIR, they found that the MWCNTs serve as templates for the conformational ordering of PLLA by providing reactive surfaces on which strong noncovalent

Scheme 1. Schematic Diagrams of Conformational Ordering on theMWCNT Surface: (a) Melt State, (b) Early Stage, and (c) Later Stage

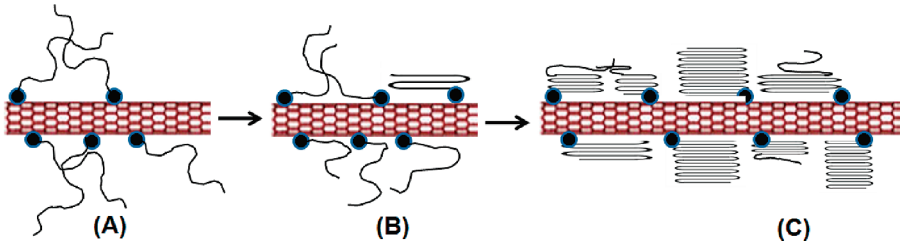

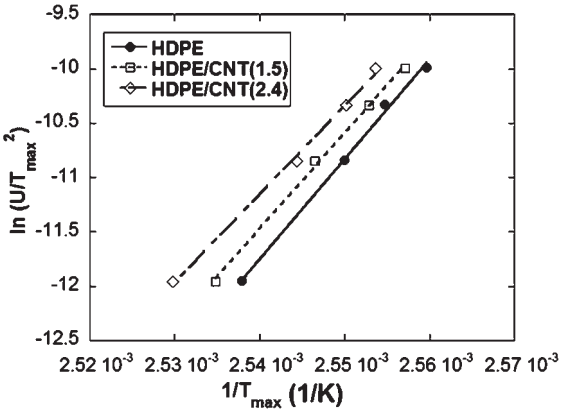

Figure 8. Determination of the activation energy describing the nonisothermal crystallization process for HDPE and MWCNT nanocomposites based on the Kissinger method.

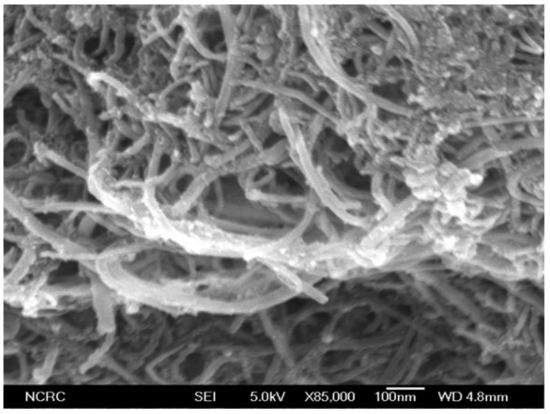

Figure 9. SEM image of HDPE/MWCNT (2.4 wt %) after a Soxhlet extraction of HDPE (magnification ×45 000).

binding with polymer chains can occur. They used a solution coagulation method to prepare the PLLA/CNT nanocomposites. They observed free PLLA molecules to change their orientation from a random rearrangement in the solution to an in-plane orientation, thus displaying a unique template effect of carbon nanotubes or to the conformational ordering of PLLA. However, this result is for the crystallization of free molecules on the MWCNT surface and is different from the current case in which PE molecules produced by an *in situ* polymerization process are rooted on the MWCNT surface. As the PE grows up, it wraps the MWCNTs. Hence, MWCNTs are not expected to interact with each other to form aggregates. Figure 9 shows MWCNTs after the HDPE moiety was dissolved by boiling dichlorobenzene for a week in a Soxhlet extract. The larger radii than primitive MWCNT radii that are observed after treatment with the dichlorobenzene explicitly indicate that MWCNTs are totally wrapped by HDPE.

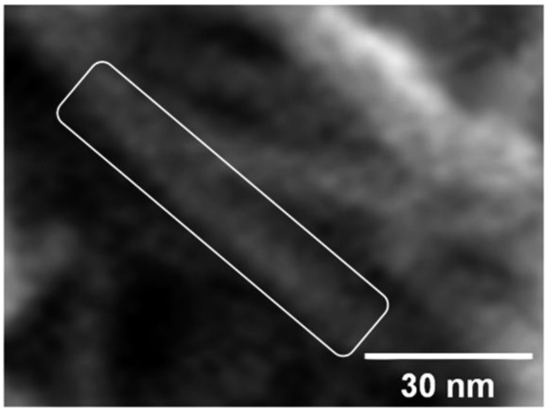

Figure 10. Enlarged SEM image of HDPE/MWCNT (2.4 wt %) after Soxhlet extraction of HDPE. The rectangular section shows the disk-shaped PE crystals around the carbon nanotubes.

Considering all of these results, we can describe the crystallization process as follows: the chains rooted on the MWCNT surface crystallize along the surface. The −CH group of the polymers allows for the CH−π interaction,[43] and successive −CH groups gradually attach themselves to the surface, leading to parallel chain adsorption (Scheme1). Considering the curvature of the MWCNTs, the HDPE molecules preferentially align themselves parallel to the nanotube axis. Upon crystallization, the PE crystallites nucleate on the MWCNTs and grow parallel to the nanotubes. Depending on each HDPE molecule's molar mass and frequency of neighboring crystallites, the HDPE grows perpendicular to MWCNT surface. Primitive growth on the MWCNTs forms nanotubes wrapped by HDPE molecules, whose shape is similar to shish of a shish-kebab morphology of melt-spun polyethylene fibers. Figure 10 shows the shish-kebab morphology of the nanocomposite. However, later ordering is difficult because of chain entanglements in nonordered moieties. The chain's movement is much slower than that of the free chains. This evidently slows down the ordering of the chains. The steps in this process can be further corroborated by closely looking at the change in the Avrami exponent with the cooling rates. As the cooling rate increases, the Avrami index decreases (Table 3). If the cooling rate is faster, then less time is necessary for a molecule to be relaxed and ordered. Thus, crystallites formed at high cooling rates imply that crystallization occurs at an earlier stage than that for low cooling rates. In the early stages of nanocomposite crystallization, the Avrami index values are less than 2 or close to 2, depending on the concentration of MWCNTs. This result indicates that more HDPE molecules have ordered conformation with slow cooling and that more HDPE-wrapped MWCNTs are formed with increasing concentrations of MWCNTs. This result also implies that the morphology of HDPE molecules grown vertically on the MWCNT surface will be in the lamellar form grown parallel to the nanotube

surface (long axis) in its infant stage and is later changed with the other part of the molecules that is still in amorphous state to the one that is grown vertically on the MWCNT surface. Because the density of HDPE roots on the MWCNT surface is very high, the crowded HDPE molecules cannot grow to form large kebabs, which is contrast to that of neat HDPE. Additionally, the half-crystallization time increased with the MWCNT concentration because of the ordering difficulties.

Conclusions

The nonisothermal crystallization analysis of HDPE and its nanocomposites with MWCNTs provides some important information about the crystalline structures of these materials. In the present work, a modified version of Ozawa's method proposed by us[38] was successfully applied to the analysis of DSC data for HDPE and its nanocomposites at various low cooling rates. The Avrami exponent of the pristine HDPE was close to 3, indicating that the crystallites had a spherulite structure while that of the nanocomposites was close to 2 depending on the concentration of the MWCNTs, indicating the growth of a 2-dimensional rod shape. Observation of the morphologies of these materials and crystallographic analysis confirmed these findings. The morphology of the pristine HDPE was spherulitic, whereas that of the HDPE in the nanocomposites consisted of rodlike structures. The observed behavior can be attributed to the large number of nuclei present on the surface of the MWCNTs. The lower activation energy of the HDPE nanocomposites implies faster crystallization due to the large density of nuclei in the sample. Anchoring the HDPE molecules on the MWCNT surface renders easy conformational ordering in early stages, but anchoring the roots on the MWCNT surface hinders the ordering of the molecules in later stages. Rooting the HDPE on the surface restricts movement in the later stages and decelerates the crystallization kinetics of HDPE. Thus, the half-crystallization time increased with the MWCNT concentration. This investigation confirms that templating on MWCNTs is quite effective for producing aligned PE morphologies.[45] The presented nonisothermal analysis implicitly provides information about the morphological development history and the molecular ordering in the nanocomposites.

Acknowledgment. This work was supported by Korea National Research Foundation (RIAM NR03-09, 0417-20090027 to Y. Seo), the SRC/ERC program of NRF (R11-2005-065 to Y. Seo), MIKE (ITSTD Program RIAM AC 2509, 0417-20096070, J. R. Lee), Core Technology Program by MOCIE (N.13-5060, S. M. Hong), and the Grant-in-Aid for the Global COE Program ("Science for Future Molecular Systems" (Japan), A. Takahara).

References and Notes

(1) Jin, Y.; Park, H.; Im, S. S.; Kwak, S. Y.; Kwak, S. *Macromol. Rapid Commun.* **2002**, *23*, 135.
(2) Berber, S.; Kwon, Y.-K.; Tomanek, D. *Phys. Rev. Lett.* **2000**, *84*, 4613.
(3) Yang, D. J.; Zhang, Q.; Chen, G.; Yoon, S. F.; Ahn, J.; Wang, S. G.; Zhou, Q.; Wang, Q.; Li, J. Q. *Phys. Rev. B* **2002**, *66*, 1654401.
(4) Liu, T.; Phang, I. Y.; Shen, L.; Chow, S. Y.; Zhang, W.-D. *Macromolecules* **2004**, *37*, 7214.
(5) Sánchez, S.; Pumera, M.; Fàbregas, E.; Bartrolí, J.; Esplandiu, M. J. *Phys. Chem. Chem. Phys.* **2009**, *11*, 7721.
(6) Haggenmueller, R.; Guthy, R.; Lukes, J. R.; Fischer, J. E.; Winey, K. I. *Macromolecules* **2007**, *40*, 2417.
(7) Sun, Y. P.; Fu, K.; Lin, Y.; Huang, W. *Acc. Chem. Res.* **2002**, *35*, 1096.
(8) Park, S.; et al. *Chem. Mater.* **2008**, *20*, 4588.
(9) Trujillo, M.; Arnal, M. L.; Mu1ller, A. J.; Laredo, E.; Bredeau, St.; Bonduel, D.; Dubois, Ph. *Macromolecules* **2007**, *40*, 6268.
(10) Toti, A.; Giambastiani, G.; Bianchini, C.; Meli, A.; Bredeau, S.; Dubois, Ph.; Bonduel, D.; Claes, M. *Chem. Mater.* **2008**, *20*, 3092.
(11) Bonduel, D.; Bredeau, S.; Alexandre, M.; Monteverde, F.; I.W. Dubois, Ph. *J. Mater. Chem.* **2007**, *17*, 2359.
(12) Haggenmueller, R.; Fischer, J. E.; Winey, K. I. *Macromolecules* **2006**, *39*, 2964.
(13) Trujillo, M.; Arnal, M. L.; Mu1ller, A. J.; Bredeau, T.; Bonduel, D.; Dubois, Ph.; Hamley, I. W.; Castelletto, V. *Macromolecules* **2008**, *41*, 2087.
(14) Grady, B. P.; Pompeo, F.; Shambaugh, R. L.; Resasco, D. E. *J. Phys. Chem. B* **2002**, *106*, 5852.
(15) Bhattacharyya, A. R.; Sreekumar, T. V.; Liu, T.; Kumar, S.; Ericson, L. M.; Hauge, R. H.; Smalley, R. E. *Polymer* **2003**, *44*, 2373.
(16) Anand, K. A.; Agarwal, U. S.; Joseph, R. *Polymer* **2006**, *47*, 3976.
(17) Du, F.; Fischer, J. E.; Winey, K. I. *J. Polym. Sci., Part B: Polym. Phys.* **2003**, *41*, 3333.
(18) Srivastava, D.; Brenner, D. W.; Schall, J. D.; Ausman, K. D.; Yu, M.; Ruoff, R. S. *J. Phys. Chem. B* **1999**, *103*, 4330.
(19) Niyogi, S.; Hamon, M. A.; Hu, H.; Zhao, B.; Bhowmik, P.; Sen, R.; Itkis, M. E.; Haddon, R. C. *Acc. Chem. Res.* **2002**, *35*, 1105.
(20) Li, L.; Li, C. Y.; Ni, C. *J. Am. Chem. Soc.* **2006**, *128*, 1692.
(21) Kodjie, S. L.; Li, L.; Li, B.; Cai, W.; Li, C. Y.; Keating, M. *J. Macromol Sci., Part B: Phys.* **2006**, *45*, 231.
(22) Assouline, E.; Lustiger, A.; Barber, A. H.; Cooper, C. A.; Klein, E.; Wachtel, E.; Wagner, H. D. *J. Polym. Sci., Part B: Polym. Phys.* **2003**, *41*, 520.
(23) Minus, M. L.; Chae, H. G.; Kumar, S. *Polymer* **2006**, *47*, 3705.
(24) Michell, C. A.; Krishnamoorti, R. *Polymer* **2005**, *46*, 8796.
(25) Li, L.; Li, B.; Hood, M.; Li, C. Y. *Polymer* **2009**, *50*, 953.
(26) Bonduel, D.; Mainil, M.; Alexandre, M.; Monteverde, F.; I.W. Dubois, Ph. *Chem. Commun.* **2005**, 781.
(27) Jeon, K.; Lumata, L.; Tokumoto, T.; Steven, E.; Brooks, J.; Alamo, R. G. *Polymer* **2007**, *48*, 4751.
(28) Kim, J.; Hong, S. M.; Kwak, S.; Seo, Y. *Phys. Chem. Chem. Phys.* **2009**, *11*, 10851.
(29) Ozawa, T. *Polymer* **1971**, *12*, 150.
(30) Nakamura, N.; Watanabe, T.; Kotayama, K.; Amano, T. *J. Appl. Polym. Sci.* **1972**, *16*, 1077.
(31) Evans, U. R. *Trans. Faraday Soc.* **1941**, 365.
(32) Srinivas, S.; Babu, J. R.; Riffle, J. S.; Wilkes, G. L. *Polym. Eng. Sci.* **1997**, *37*, 497.
(33) Cebe, P.; Hong, S. *Polymer* **1986**, *27*, 1183.
(34) Seo, Y.; Kim, S. *Polym. Eng. Sci.* **2001**, *41*, 940.
(35) Seo, Y.; Kang, T.; Hong, S. M.; Choi, H. J. *Polymer* **2007**, *48*, 3844.
(36) Peacock, A. J. *Handbook of Polyethylene, Structures, Properties, and Applications*; Marcel Dekker: New York, 2000; pp 376−382.
(37) Watts, P. C. P.; Fearon, P. K.; Hsu, W. K.; Billingham, N. C.; Kroto, H. W.; Walton, D. R. M. *J. Mater. Chem.* **2003**, *13*, 491.
(38) Seo, Y. *Polym. Eng. Sci.* **2000**, *40*, 1293.
(39) Sperling, L. H. *Physical Polymer Science*; John Wiley & Sons: New York, 2001; Chapter 6.
(40) Wunderlich, B. In *Thermal Characterization of Polymeric Materials*; Turi, A., Ed.; Academic Press: New York, 1997; Chapter 2.
(41) Kissinger, H. E. *J. Res. Natl. Bur. Stand.* **1956**, *57*, 217.
(42) Chen, X.; Wang, L.; Liu, Y.; Shi, J.; Shi, H. *Polym. Eng. Sci.* **2009**, *50*, 2342.
(43) Anand, K. A.; Aggarwal, U. S.; Joseph, R. *Polymer* **2003**, *44*, 2373.
(44) Yang, J.; Wang, K.; Deng, H.; Chen, F.; Fu, Q. *Polymer* **2010**, *51*, 774.
(45) Hu, X.; An, H.; Li, Z.; Geng, Y.; Li, L.; Yang, C. *Macromolecules* **2009**, *42*, 3215.